Colloid Polym Sci (2008) 286:1613–1619
DOI 10.1007/s00396-008-1935-6

ORIGINAL CONTRIBUTION

Rheological behavior of viscoelastic wormlike micelles in mixed sodium dodecyl trioxyethylene sulfate–monolaurin aqueous system

Suraj Chandra Sharma · Rekha Goswami Shrestha · Lok Kumar Shrestha · Kenji Aramaki

Received: 23 July 2008 / Revised: 15 September 2008 / Accepted: 22 September 2008 / Published online: 16 October 2008

Abstract Rheological behavior of viscoelastic wormlike micelles in an aqueous system of mixed sodium dodecyl trioxyethylene sulfate (SDES)–monolaurin (ML) is presented. Dilute aqueous solution of SDES has a high fluidity and follows Newtonian liquid-like behavior due to formation of small globular type of micellar structure. Addition of lipophilic nonionic cosurfactant ML to dilute or semidilute solution of SDES decreases the interfacial curvature of the aggregates favoring one dimensional micellar growth, and hence, viscosity increases. After a certain concentration of ML, the elongated micelles get entangled with each other leading to the formation of viscoelastic wormlike micelles. The viscoelastic solution follows Maxwell model of a single stress relaxation mode at low-frequency region. Further addition of ML decreases the viscosity of the solution due to formation of micellar joints in the network structure. The viscosity of the viscoelastic wormlike micelles decreases upon heating, and the system with poor viscoelastic character is observed at higher temperatures.

Keywords Sodium dodecyl trioxyethylene sulfate · Monolaurin · Rheology · Wormlike micelles · Viscoelasticity

S. C. Sharma
Department of Pure and Applied Chemistry,
Faculty of Science and Technology, Tokyo University of Science,
2641 Yamazaki, Noda,
Chiba 278-8510, Japan

R. G. Shrestha · L. K. Shrestha · K. Aramaki (✉)
Graduate School of Environment and Information Sciences,
Yokohama National University,
Tokiwadai 79-7, Hodogaya-ku,
Yokohama 240-8501, Japan
e-mail: aramakik@ynu.ac.jp

Introduction

It is well known that in aqueous solutions of long-chain cationic surfactants, such as hexadecyltrimethyl ammonium bromide, wormlike micelles are formed upon addition of counterions such as salicylate or bromide ions [1–7]. The counterions serve to reduce the electrostatic interactions between the cationic head groups, thus, reducing the interfacial curvature of the aggregates and thereby promoting the one dimensional micellar growth. At certain concentrations, wormlike micelles typically become entangled into a transient network, thereby imparting viscoelastic properties [8] analogous to that observed in flexible polymer solutions. Several reports on the formation of viscoelastic wormlike micelles in mixed cationic–anionic, ionic–nonionic, and in some cases, in zwitterionic surfactant systems are available in the literature [9–14]. There are ample of recent reports on wormlike micelles in mixed nonionic surfactants system [15–19]. To the best of our knowledge, much less is known, in comparison, regarding the formation and rheological behavior of the wormlike micelles in anionic surfactants system. Usually, anionic surfactants are biodegradable and less toxic compared to cationic ones and are, therefore, considered to be more environmentally friendly [20]. Hence, the formation of wormlike micelles in the anionic surfactant could offer many advantages in cosmetics, toiletry, and pharmaceutical formulations.

Sodium dodecyl trioxyethylene sulfate (SDES) represents a class of surfactants widely used in the formation of personal care and household cleaning products due to its superb foaming properties and low price. Hence, the study of the rheological properties of wormlike micelles in this system is essential. Mu et al. [21–23] studied the viscoelastic properties of wormlike micelles in SDES aqueous solution with multivalent cations such as Al^{3+},

Mg^{2+}, Ca^{2+}, and Na^+. Recently, Aramaki et al. [24, 25] observed the cosurfactant-induced micellar growth in the same system. In order to enrich the knowledge about the rheological properties of wormlike micelles formed by SDES system in an aqueous solution, we decided to extend the further study with monolaurin (ML) to fill this gap.

The paper at hand reports the rheological behavior of the viscoelastic wormlike micellar solutions in the aqueous system with mixed anionic surfactant (SDES) and ML. At first, we present a partial phase diagram water–SDES–ML system at 25 °C. Next; we discuss the effect of cosurfactant concentration on the rheological properties at constant concentration of SDES. Finally, effect of temperature on the rheology of viscoelastic wormlike micelles is explained.

Experimental

Materials

An aqueous solution of sodium dodecyl trioxyethylene sulfate $CH_3(CH_2)_{10}CH_2(OCH_2CH_2)_3OSO_3^-Na^+$ (abbreviated as SDES) containing 24.7 wt.% of the surfactant was obtained from Kao Corporation, Japan. ML was purchased from Tokyo Chemical Industry Co., Ltd. Japan. All the chemicals were used as received. Millipore water was used throughout the experiment.

Phase diagram

Samples for phase diagram construction were prepared by weighing the required amounts of reagents into test tubes fitted with screw cap and mixed using a vortex mixer. The samples were kept in a water bath at 25 °C for equilibration. Phases were identified by visual observation (through crossed polarizer).

Rheological measurements

Samples for rheological measurements were homogenized and kept in water bath at specified temperature for at least 24 h to ensure equilibration before performing measurements. The rheological measurements were performed in a stress-controlled rheometer, AR-G2 (TA Instrument), using cone-plate geometries (diameters 60 mm for low-viscosity sample and 40 mm for high-viscosity sample, each with a cone angle of 1°) with the plate temperature controlled by peltier unit. A sample cover provided with the instrument was used to minimize the change in sample composition by evaporation during the measurement. Frequency sweep measurements were performed in the linear viscoelastic regime of the samples, as determined previously by dynamic strain sweep measurements. The zero-shear viscosity of the samples was determined either from steady shear rate measurement of less viscous samples by extrapolating the viscosity versus shear-rate curve to zero shear-rate or from the values of G_o and τ_R (see Eq. 3) as obtained from oscillatory measurements.

Results and discussion

Phase behavior

A partial ternary phase diagram of water/SDES/ML system at 25 °C is shown in Fig. 1. In the water–SDES binary system, an isotropic micellar solution (W_m) is formed up to the maximum concentration of SDES (24.7 wt.%) at 25 °C. The micellar solution of SDES can solubilize a significant amount of ML, which is reflected from the micellar (W_m) domain in the ternary phase diagram. Incorporation of ML in the micellar aggregates of SDES reduces average head group area at the interface or, in other words, reduces the interfacial curvature, and beyond the solubilization limit of the W_m phase, the L_α phase separates out from the isotropic solution. Upon successive addition of ML to the micellar solution of SDES in the dilute region, no significant change in viscosity occurs, but as the surfactant concentration increases (≥10 wt.% of SDES), addition of ML increases viscosity gradually at first, then rapidly, and a viscous solution is observed. The viscous solutions are isotropic at rest but are birefringent when applied a shear, such as a sudden jerk. With further addition of ML, viscosity decreases, and ultimately, a phase separation occurs. The shaded area in the phase diagram indicates the tentative viscous region inside W_m phase. The present surfactant, SDES shows similar phase behavior in ternary mixtures of SDES–water–alkanolamides or SDES–water–polyoxyethylene dodecyl ether as reported by Aramaki

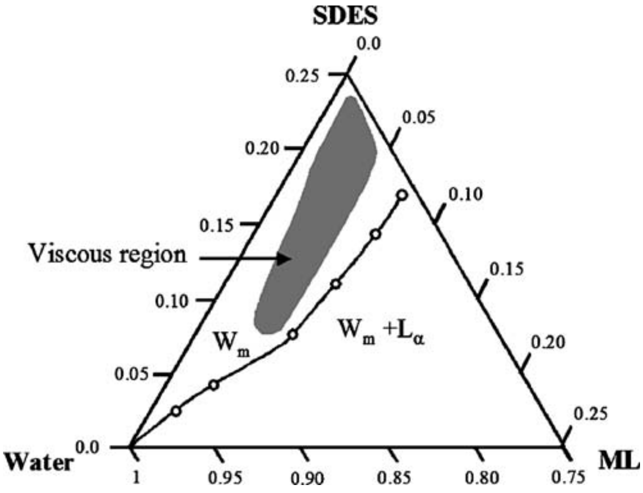

Fig. 1 Partial ternary phase diagram of water/SDES/ML system at 25 °C. W_m stands for the isotropic micellar solution, and L_α is the lamellar liquid crystalline phase

et al. [24, 25]. However, a wider viscous region of viscoelastic wormlike micelles is observed with ML in the present system.

Rheological behavior

Effect of surfactant concentrations

Figure 2 shows the steady shear-rate ($\dot{\gamma}$)-viscosity (η) curves for 10 wt.% SDES + ML systems at different mixing fraction of ML, expressed in weight fraction of ML in total surfactant (W_s) at 25 °C. At lower value of W_s, η is independent of $\dot{\gamma}$, i.e., Newtonian flow behavior is observed up to $\dot{\gamma} = 1,000\,\mathrm{s}^{-1}$. At $W_s \approx 0.24$, behavior is still Newtonian over wide range of shear rate, but a small shear thinning occurs at large deformation ($\dot{\gamma} \geq 100\,\mathrm{s}^{-1}$). With increasing W_s say up to $W_s \approx 0.32$, the critical shear rate, $\dot{\gamma}_c$ (the shear rate at which shear thinning occurs) shifts gradually to lower values and also the viscosity in the plateau region (low $\dot{\gamma}$ region) increases showing that the system is getting more structured. In fact, the samples are viscoelastic near this composition. However, with further increase in ML concentration (at $W_s \approx 0.35$) the viscosity decreases and higher deformation rate is required to induce shear thinning. This indicates structural transformation occurs after the viscosity maximum. One possibility is that the system becomes less structured, i.e., micellar length decreases and gradually network structure is lost. However, such structural changes do not seem to be convincing because the interfacial curvature should be continuously decreasing with increasing ML concentration, and aggregates with flat bilayer are formed finally at phase separation.

A more credible explanation for the change in the rheological behavior is that with increasing W_s, the spontaneous interfacial curvature of aggregate gradually decreases and, as a result, energy required for the formation of hemispherical end caps of the cylindrical micelles increases. The end-cap energy can be minimized only if the free ends fuse with cylindrical part of its own or other micelles, thus, forming micellar joints or branching in the network structure [26]. Such joints reduce the viscosity because when a stress is applied, micellar joint can slide along the cylindrical body (contour), thereby allowing a fast stress relaxation process. In some surfactant systems, micellar connections or branching points have been detected by cryogenic transmission electron microscopy, especially in the region where the viscosity decreases after the maximum [27–30]. Steady-shear measurements on 15 wt.% SDES + ML systems show a similar trend with increasing concentration of ML. The Newtonian behavior is noticed at low ML concentration, while shear thinning is observed at high ML concentration.

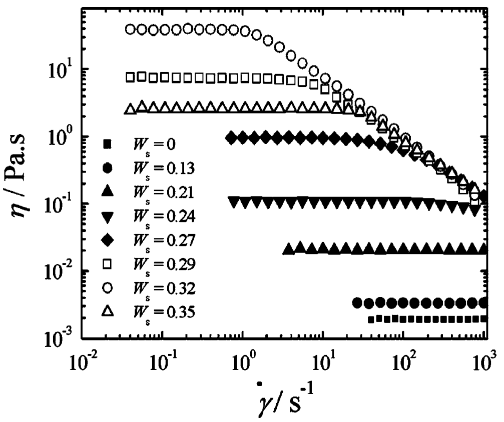

Fig. 2 Steady shear-rate ($\dot{\gamma}$)–viscosity (η) curves for 10 wt.% SDES + ML systems at various mixing fraction of ML in total surfactant, W_s. The measurements were carried out at 25 °C

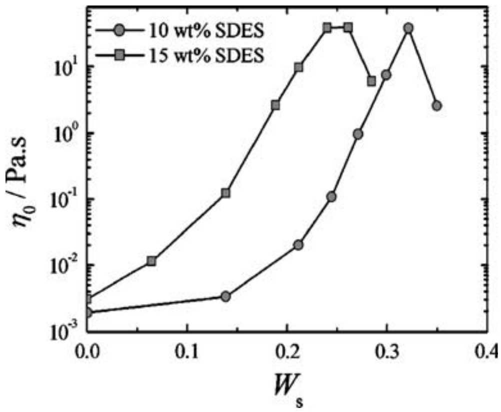

Fig. 3 Variation of zero-shear viscosity (η_0) as a function of the mixing fraction of ML in total surfactant, W_s, at two different SDES concentrations

The effect of ML concentration on the viscosity growth for the systems described in Fig. 2 can be seen more clearly in Fig. 3, where zero-shear viscosity (η_0) is plotted as a

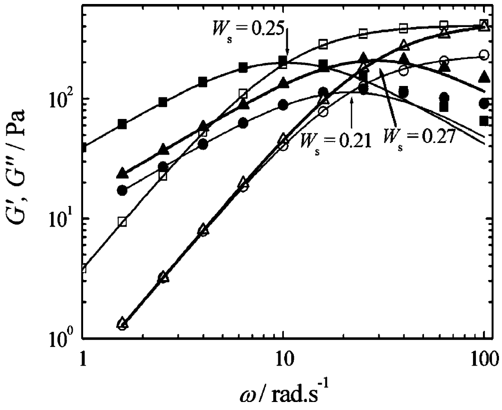

Fig. 4 Variation of elastic modulus, G' (*open symbols*) and viscous modulus, G'' (*closed symbols*) as a function of oscillatory shear frequency (ω) as obtained by frequency sweep measurement at 25 °C for 15 wt.% SDES + ML systems at different mixing fraction of ML in total surfactant, W_s. Solid lines represent the fittings to the Maxwellian equation

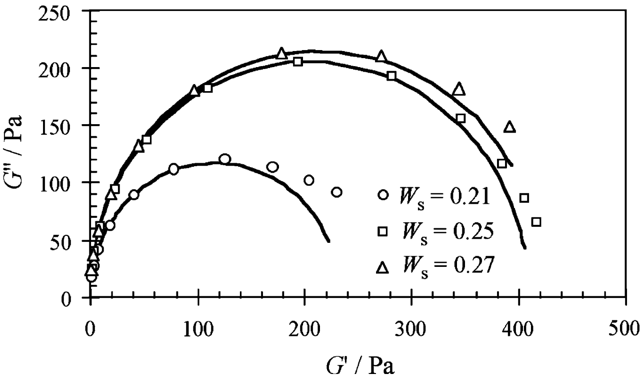

Fig. 5 Cole–Cole plots for 15 wt.% SDES + ML systems shown in Fig. 4

function of W_s. Above a certain value of W_s, the η_0 increases rapidly and attains the maximum, followed by a decline. The SDES concentration does not change the maximum value of η_0, but as the SDES concentration increases, the η_0–W_s curves shifts towards lower W_s values. In other words, small amount of ML is required to achieve comparable viscosity, which can be attributed to the decrease in the effective area a_s, of the surfactant head group at the interface with increasing SDES concentration. It is worth to compare the rheological behavior of the present system with the previously reported systems of same surfactant. The SDES forms viscoelastic wormlike micelles in aqueous systems when alkanolamides or polyoxyethylene dodecyl ether is used as cosurfactants. However, rheological behavior differs depending on the cosurfactants. The maximum zero-shear viscosity obtained in the present system is comparable to that of the SDES–water–polyoxyethylene dodecyl ether and the SDES–water–*N*-hydroxyethyl-*N*-methyldodecanamide but less than the observed with the SDES–water–*N*-hydroxyethyl-*N*-methylhexadecanamide [24, 25].

Dynamic oscillatory-shear (frequency sweep) measurements were carried out on the viscous samples. The representative plots of elastic modulus (G') and loss modulus (G'') as a function of oscillatory shear frequency (ω) for 15 wt.% SDES + ML systems at different W_s is shown in Fig. 4. The arrows highlight the intersection point of G' and G''.

The dynamic rheology data show that samples exhibit viscoelastic character in the timescale of measurement, with $G'<G''$ in low-ω region and $G'>G''$ in high-ω region. This viscoelastic behavior is attributed to the entanglement of wormlike micelles to form a transient network structure. In the low-ω region, the data points of G' and G'' fits well to following Maxwell's mechanical model of viscoelastic material described by the Eqs. 1 and 2, which considers a single process for stress relaxation, characterized by parameter τ_R called relaxation time.

$$G'(\omega) = \frac{\omega^2\tau_R^2}{1+\omega^2\tau_R^2} G_o \tag{1}$$

$$G''(\omega) = \frac{\omega\tau_R}{1+\omega^2\tau_R^2} G_o \tag{2}$$

As it is evident from the Maxwell equations, at low-frequency region $\omega <<\omega_c$, G' and G'' scale with ω according to $G'\sim\omega^2$ and $G''\sim\omega$. In the high-frequency region or, more specifically, in the region of $\omega>>\omega_c$, however, G' attains a plateau value equal to G_o whereas G'' shows a monotonic decrease. The shear frequency corresponding to G'–G'', crossover ω_c is equal to the inverse of τ_R. Considering reptation or diffusion of wormlike micelles along its own contour as the mechanism of stress relaxation in the entangled network, as proposed by Cates et al., the magnitude of τ_R is related to the average length of the wormlike micelles, whereas G_o is related to the number density of entanglement in the transient network [31, 32]. The parameters G_o and τ_R are related to η_o by the Eq. 3.

$$\eta_o = G_o\,\tau_R \tag{3}$$

Maxwellian mechanical model describes the rheological behavior in the low-ω region, but at high-ω region, the experimental data show a significant deviation, which is generally considered to be due to faster relaxation processes such as Rouse modes [31].

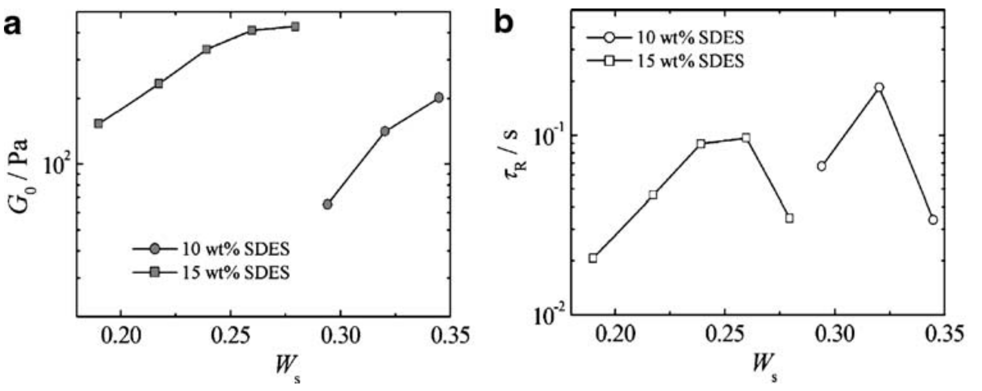

Fig. 6 **a** Variation of shear modulus (G_o) as a function of the mixing fraction of ML in total surfactant (W_s) at different SDES composition at 25 °C and **b** the corresponding relaxation time (τ_R). The *solid lines* are visual guide

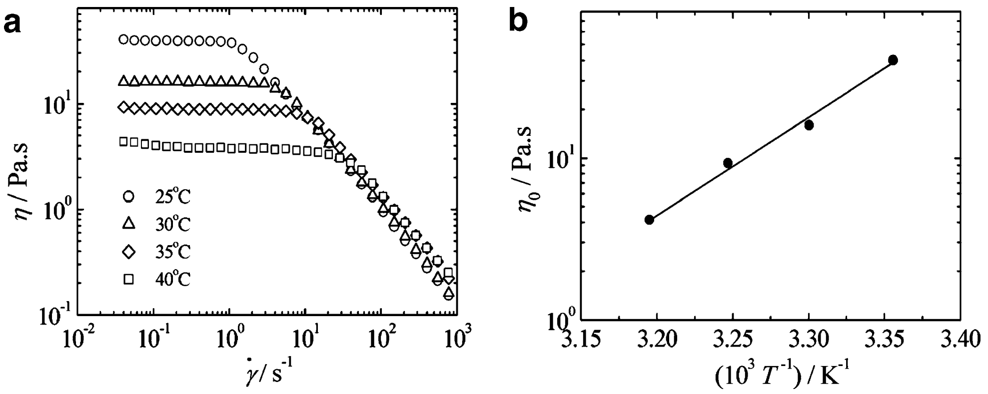

Fig. 7 Variation of (**a**) viscosity (η) with shear rate ($\dot{\gamma}$) at different temperatures and (**b**) zero-shear viscosity (η_o) with $1/T$ in a semilog (Arrhenius) plot for 10 wt.% SDES + ML (W_s=0.32) system

As it can be seen from Fig. 4, with increasing W_s, the frequency at which the G' and G'' cross shifts towards lower value and attains the lowest value at a composition corresponding to viscosity maximum (W_s=0.25). With further increasing concentration of ML, the crossover frequency, ω_c, (the frequency at which G' and G'' cross) finally shifts towards the higher value indicating a faster stress relaxation with poorer viscoelastic behavior. The good fitting of Maxwell model to the experimental data is sometimes difficult to be determined. A Cole–Cole plot (plot of G'' as a function of G') can easily visualize how well the data fits to Maxwell model. The Cole–Cole plots of the 15 wt.% SDES + ML systems at different W_s are presented in Fig. 5. The experimental data points closely follow Maxwell behavior with a semicircular behavior in the Cole–Cole plot.

Figure 6 shows the variation of rheological parameters G_o and τ_R as function of W_s. These parameters are obtained by fitting of the experimental data from frequency sweep measurements, especially the data in low-frequency region, to the Maxwell equations. As in the case of the systems described in Fig. 4, G' at the high-ω region (say G'_{∞}) is often higher than perfect plateau value (G_o) as predicted by Maxwell equations. Therefore, the values of G_o estimated from Maxwell equations should be considered as the lower limit for the shear modulus.

The shift of the η_o and τ_R curves toward the lower W_s values in the η_o–W_s (Fig. 3) and τ_R–W_s (Fig. 6b) plots upon increasing the SDES concentration in the mixed system corresponds to the higher extent of linear micellar growth. This is also evident from the increase in G_o or network density upon increasing surfactant concentration (Fig. 6a). The lower value of τ_R at the maximum in 15 wt.% SDES + ML systems in comparison to that in 10 wt.% SDES + ML systems should not be considered as a lower extent of micellar growth in the former system. Instead, it might have arisen from the fact that with increasing surfactant concentration the spontaneous curvature decreases and the system favors micellar branching even at lower value of W_s so as to minimize energy cost of the formation of end caps. Continuous increase of G_o in the given composition range where η_o and τ_R decrease after a certain ML concentration shows that after branching the network density grows until the phase separation occurs. There are indications that the local structure at branching points evolve toward bilayer structure and ultimately separates out.

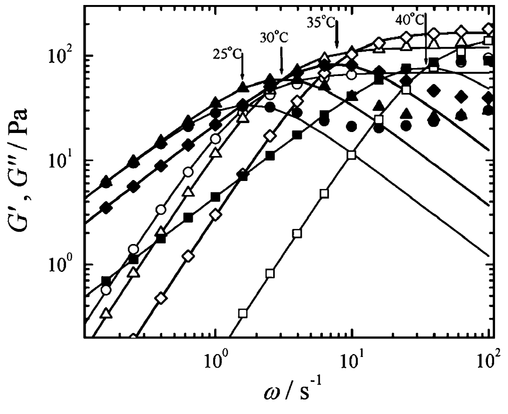

Fig. 8 Variation of elastic modulus, G' (*open symbols*) and viscous modulus, G'' (*closed symbols*) as a function of oscillatory shear frequency (ω) as obtained by frequency sweep measurement at different temperatures. The sample composition is fixed to 10 wt.% SDES + ML (W_s=0.32). *Circles* (25 °C), *triangles* (30 °C), *diamond* (35 °C), and *squares* (40 °C). *Solid lines* represent the fittings to the Maxwellian equation

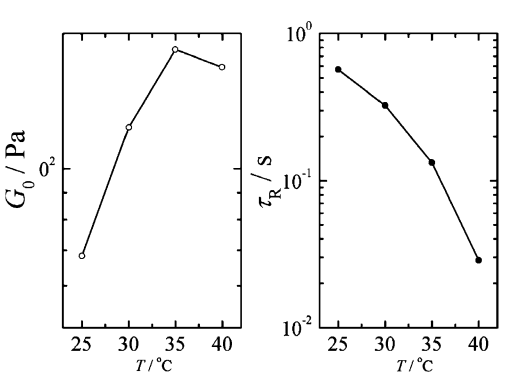

Fig. 9 Shear modulus (G_o) (*left*) and relaxation time (τ_R) (*right*) at different temperatures. The sample composition is fixed to 10 wt.% SDES + ML (W_s=0.32). The *solid lines* are visual guide

Effect of temperature

Temperature is a key parameter having major influence on the micellar structure and the rheological behavior of wormlike micellar solution. In poly(oxyethylene) type nonionic aqueous surfactant systems, temperature effect is pronounced. Namely, as we increase temperature, the micellar length increases due to dehydration of oxyethylene unit and consequently viscosity increases. Compared to the nonionic surfactant systems, temperature effect is less pronounced in the ionic surfactant systems. Figure 7 shows the effect of temperature on the steady shear rheology of 10 wt.% SDES + ML (W_s=0.32) system. The data show that the samples become less viscous upon heating. The critical shear rate $\dot{\gamma}_c$ increases with increasing temperature. The value of $\dot{\gamma}_c$ increases by approximately one order of magnitude upon increasing temperature from 25 to 40 °C (see Fig. 7a). On the other hand, the zero-shear viscosity decreases exponentially with temperature as proven by the Arrhenius plot of log η_o versus $1/T$ in Fig. 7b. This exponential decay of viscosity with temperature is in accordance with the well-known Eq. 4 for wormlike micelles [32, 33].

$$\eta_0 = Ae^{\frac{E_a}{RT}} \tag{4}$$

where E_a is the flow activation energy, R is the universal gas constant, and A is a constant. The value of flow activation energy is calculated to 125.3 kJ/mol from the slope of the straight line fit in the Fig. 7b. This value of flow activation energy lies in the range of 70–300 kJ/mol reported values for other wormlike micelles in other systems [33–37]. The exponential decay in the viscosity with temperature may be due to the formation of the micellar joints in the network structure [33, 38].

The effect of temperature on the oscillatory-shear rheological behavior of a viscoelastic sample with composition 10 wt.% SDES + ML (W_s=0.32) is presented in Fig. 8. The data points of G' and G'' can be well fitted to the Maxwell model with a single relaxation at lower frequencies. With increasing temperature, the entire frequency spectrum shifts to the right (i.e., to higher frequencies). The shift in crossover frequency ω_c to higher value indicating that the relaxation time τ_R decreases with temperature; hence, the system exhibits less viscoelastic character.

With increasing temperature, G_o shows a monotonic increase up to a certain temperature (35 °C) and after that, it decreases slightly (see Fig. 9). On the other hand, τ_R decreases continuously with rise in temperature. Since the density of the entanglements of the wormlike micelles increases with increasing temperature (up to 35 °C), the decrease in viscosity with temperature (up to 35 °C) can be attributed to the micellar branching. Above this temperature, the reason of micelles shortening for the drop in viscosity seems to be plausible as G_o decreases.

Summary

Rheological behavior of viscoelastic wormlike micelles formed in an aqueous solution of mixed SDES and ML is reported. Addition of lipophilic nonionic cosurfactant ML to the semidilute solution of SDES reduces the interfacial curvature of the aggregates and induces one dimensional micellar growth. With successive addition of the ML, viscosity increases rapidly to form viscoelastic solution. After the maximum viscosity is achieved, further addition of ML leads to viscosity decrease due to branching of wormlike micelles and ultimately a phase separation occurs. The dynamic rheological behavior of the viscoelastic solution can be described by Maxwell model at low-frequency region, which is typical behavior of wormlike micelles. Increasing temperature decreases the viscosity and the system with poor viscoelastic character is observed at higher temperatures.

Acknowledgement S.C.S. and L.K.S. are thankful to Japan Society for the Promotion of Science for financial support.

References

1. Kern F, Lemarechal P, Candau SJ, Cates ME (1992) Langmuir 8:437
2. Khatory A, Lequeux F, Kern F, Candau SJ (1993) Langmuir 9:1456
3. Kim WJ, Yang SM, Kim M (1997) J Colloid Interface Sci 194:108
4. Kim WJ, Yang SM (2000) J Colloid Interface Sci 232:225
5. Imai S, Shikata T (2001) J Colloid Interface Sci 244:399
6. Vethamuthu MS, Almgren M, Brown W, Mukhtar E (1995) J Colloid Interface Sci 174:461
7. Hartmann V, Cressely R (19979) Colloids Surf A 121:151
8. Lin Z, Cai JJ, Scriven LE, Davis HT (1994) J Phys Chem 98:5984
9. Schubert BA, Kaler EW, Wagner NJ (2003) Langmuir 19:4079
10. Kunieda H, Rodríguez C, Tanaka Y, Kabir MH, Ishitobi M (2004) Colloids Surf B 38:127
11. Rodríguez C, Acharya DP, Hattori K, Sakai T, Kunieda H (2003) Langmuir 19:8692
12. Acharya DP, Hattori K, Sakai T, Kunieda H (2003) Langmuir 19:9173
13. Hoffmann H, Rauscher A, Gradzielski M, Schulz SF (1992) Langmuir 8:2140
14. Kumar R, Kalur GC, Ziserman L, Danino D, Raghavan SR (2007) Langmuir 23:12849
15. Acharya DP, Kunieda H (2003) J Phys Chem B 107:10168
16. Acharya DP, Hossain MK, Feng J, Sakai T, Kunieda H (2004) Phys Chem Chem Phys 6:1627
17. Naito N, Acharya DP, Tanimura K, Kunieda H (2004) J Oleo Sci 53:599
18. Sharma SC, Acharya DP, Aramaki K (2007) Langmuir 23:5324

19. Maestro A, Acharya DP, Furukawa H, Gutiérrez JM, López-Quintela MA, Ishitobi M, Kunieda H (2004) J Phys Chem B 108:14009
20. Kalur GC, Raghavan SR (2005) J Phys Chem B 109:8599
21. Mu JH, Li GZ (2001) Colloid Polym Sci 279:872
22. Mu JH, Li GZ (2001) Chem Phys Lett 345:100
23. Mu JH, Li GZ, Jia XL, Wang HX, Zhang GY (2002) J Phys Chem B 106:11685
24. Varade D, Sharma SC, Aramaki K (2007) J Colloid Interface Sci 313:680
25. Acharya DP, Varade D, Aramaki K (2007) J Colloid Interface Sci 315:330
26. Candau SJ, Oda R (2001) Colloids Surf A 183–185:5
27. Lin Z (1996) Langmuir 12:1729
28. Danino D, Talmon Y, Levy H, Beinert G, Zana R (1995) Science 269:1420
29. In M, Aguerre-Chariol O, Zana R (1999) J Phys Chem B 103:7747
30. Zana R (2002) Adv Colloid Interface Sci 97:205
31. Granek R, Cates ME (1992) J Chem Phys 96:4758
32. Cates ME, Candau SJ (1990) J Phys Condens Matter 2:6869
33. Raghavan SR, Kaler EW (2001) Langmuir 17:300
34. Oda R, Narayanan J, Hassan PA, Manohar C, Salkar RA, Kern F, Candau SJ (1998) Langmuir 14:4364
35. Makhloufi R, Cressely R (1992) Colloid Polym Sci 270:1035
36. Shrestha RG, Shrestha LK, Aramaki K (2007) J Colloid and Interface Sci 311:276
37. Shrestha RG, Shrestha LK, Aramaki K (2008) J Colloid and Interface Sci 322:596
38. Kalur GC, Frounfelker BD, Cipriano BH, Norman AI, Raghavan SR (2005) Langmuir 21:10998